

Rational Design of Diphenyldiacetylene-Based Fluorescent Materials Enabling a 365-nm Light-Initiated Topochemical Polymerization

 Mingjie Zhu and Liangliang Zhu*^[a]

Abstract: Photopolymerization of diacetylenes usually requires stringent reaction conditions like high energy irradiation of 254-nm light or even γ -rays, which are generally harmful to the human body and thus mild conditions with lower energy irradiation are required. In this study, different diphenyldiacetylene (DPDA) derivatives were rationally designed followed by the investigation of their photopolymerization behavior. It was found that the para-substituted amino groups could render the absorption band of DPDA bath-

ochromically shifted, ensuring a 365-nm light wavelength coverage. On this basis, an organogel system was constructed by chemically modifying cholesteryl and lipoic acid onto the DPDA moiety in aromatic solvents. Such uniform self-assemblies further facilitated to a rather high degree of polymerization by 365-nm irradiation. As a kind of fluorescent materials, the whole polymerization process of this system can be visualized by a photoluminescent signal.

Introduction

Polydiacetylenes (PDAs) are usually fabricated through topochemical reaction initiated remotely without any additives. The well-defined alternating ene-yne conjugated skeleton allows the resulting materials to exhibit fascinating optical^[1] and electrical^[2] properties like chromatism and semi-conductivity, providing versatile prototypes for applications in cell imaging,^[3] photo-patterning,^[4] anti-counterfeiting,^[5] information encryption,^[6] photocatalysis,^[7] optoelectronic devices,^[8] etc. Besides, comprehensive works have also been reported by Prof. Juyoung Yoon,^[9] Prof. Jong-Man Kim^[10] and others,^[11] where various aliphatic PDAs are widely functionalized to be used as chemo/bio sensors since conventional PDAs usually go through a significant blue-to-red colorimetric transition as well as a non-fluorescent to fluorescent transition upon external stimuli.

Diphenyldiacetylene (DPDA) has received considerable attention for its uniqueness such as an extended π -conjugation structure relative to bare diacetylenes (DAs), along with a larger intermolecular stacking tendency. Although Wegner had demonstrated the topochemical reactivity of DPDA as far back as 1971,^[12] however, successful cases on polymerization of such aromatized derivatives received far less coverage in contrast with massive reports on conventional PDAs, probably due to a more stringent condition for conformational change in the molecular level. It has been generally acknowledged that the pre-arrangement of monomers is crucial to perform the 1,4-addition topochemical transformation for polymerization either

by irradiation or by heat. To be specific, crystal structures with a tilt angle of 45° relative to the diacetylene axis, and a spacing distance of 4.9 Å between two repeating units, are necessary.^[13] Yet, the bulky phenyl rings at both ends enhance the rigidity of DPDA molecular structures and obstruct the formation of alternating ene-yne bonds greatly. So far, much effort has been devoted to aligning DA monomers into such ordered systems as Langmuir-Blodgett films,^[14] crystals,^[15] liquid crystals,^[16] monolayers,^[17] gels,^[18] self-assemblies,^[19] and sacrificial templates like porous materials^[20] and block copolymers,^[21] relying on various noncovalent interactions^[22] including π - π stacking,^[23] coordination bond,^[24] intermolecular hydrogen bond,^[25] hydrophobic interaction^[26] and electrostatic interaction^[27] to maintain an ordered structure. To the best of our knowledge, most of these strategies were generally conducted by heating, 254-nm light or even γ -ray irradiation, with only a few reports concerning the topochemical reaction of aliphatic DAs initiated under 365-nm light.^[28] Unfortunately, such a relatively mild condition to trigger the topochemical polymerization of DPDA has remained less explored. In particular, the topochemical transformation process of DPDA is characterized by a distinctive photoluminescence enhancement as a result of the enlarged π -conjugated skeleton, endowing the corresponding polymeric species with prospective applications as fluorescent materials.

In this work, we aim to rationally design a pure organic material to attend this goal. Three types of DPDA derivatives containing ester or amide groups in para- or meta-position were designed (see Figure 1) for an absorption-band comparison. It is believed that to strengthen the electron-donating effect with an extended π -conjugation in DPDA can be helpful to shift its absorption bands bathochromically, ensuring a 365-nm light wavelength coverage. Cholesterol and (*R*)- α -lipoic acid have been widely used as highly efficient components to construct chiral low molar-mass organic gel^[29] with no interference with the chromophore. Moreover, organogel systems, where the reactants are aligned at proximity, are considerably

[a] M. Zhu, Prof. L. Zhu
 State Key Laboratory of Molecular Engineering of Polymers
 Department of Macromolecular Science
 Fudan University
 Shanghai 200438 (P. R. China)
 E-mail: zhuliangliang@fudan.edu.cn

Supporting information for this article is available on the WWW under <https://doi.org/10.1002/asia.202100468>

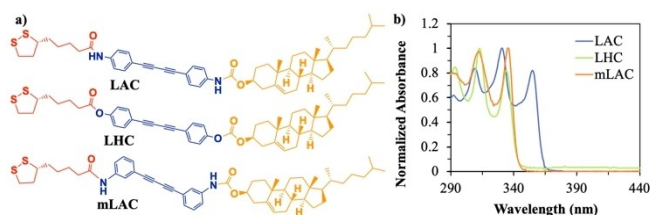


Figure 1. a) Chemical structures of the compounds in this work. b) Normalized absorption spectra measured in *p*-xylene by using quartz cuvettes with a path length of 0.1 mm at a concentration of 0.5 mM.

favorable for the pre-arrangement of monomers for topochemical transformation and polymerization.^[30] The synthesis of all compounds is detailed in the Experimental Section. We eventually found that the *para*-substituted amino groups contained monomer (LAC) can both regulate the absorption and form a chiral organogel in aromatic solvents, enabling a 365-nm light initiated topochemical polymerization as desired. Also, the reaction featured a remarkably progressive luminescence enhancement as well as a rather high degree of polymerization.

Results and Discussion

Molecular Design of the DPDA Gelators

Although the substitution of phenyl rings causes an extended π -conjugation structure in DPDA relative to bare DAs, it still fails to reach a 365-nm wavelength coverage without an appropriate further modification. To realize the supposition of photochemical reaction, the priority is to regulate the absorption of the DPDA derivatives through proper chemical modifications. Specifically, as illustrated in Figure S1, three types of DPDA molecular cores were synthesized followed by reactions with (*R*)- α -lipoic acid and cholesteryl chloroformate to afford the compounds used in this work. Figure 1b gives their normalized absorption spectra originating from the DPDA moiety (compared with Figure S2, SI). One can find that the absorption band of LAC covers longer-wavelength range than that of mLAC and LHC since a bathochromic shift of 20 nm was recorded.

Gelation Study in Selective Solvents

Organogels are known to be ideal self-assemblies with entangled three-dimensional networks for facilitating many cases of topo-polymerization in gel or xerogel state.^[31] Thus, selective solvent conditions were explored to attempt the gelation of these DPDA derivatives (see detailed results presented in Figure S3, SI). It was figured out by optimization that LAC could gel well in aromatic solvents like toluene, *p*-xylene, and *o*-xylene (Figure S4–S6, SI), with a critical gel concentration (CGC) as low as 2.0 mM in *p*-xylene. On the contrary, mLAC and LHC were found to dissolve or precipitate

in all solvents tested rather than gel (Figure S7 and S8, SI), indicative of the significance of the amide groups and substitution position for the gelation process. In addition to altering the absorption band, amide groups are expected to form intermolecular hydrogen bond and support the construction of the gel network.

Repeating the heating and cooling process of LAC always led to similar gels, indicating a reversible sol-gel transition (Figure 2a and S9, SI). The evidence of hydrogen-bond formation in LAC gel can be found by concentration-dependent ¹H NMR spectroscopy. Chemical shifts of two amide protons go downfield while the other protons remain untouched (Figure 2b and Figure S10, SI), until the concentration reaches 3.0 mM. The lack of hydrogen bond among ester groups led to the failure of LHC to gel in aromatic solvents as illustrated in ¹H NMR (Figure S12, SI). For mLAC, although the intermolecular hydrogen bond exists while monitored by the chemical shifts of amide protons (Figure S11, SI), the situation was dramatically contrary when amide groups were introduced in meta-position, leading to no gelation either. FESEM image showed that large coils with hierarchical nanostructures were formed rather than an entangled fibrous network. The difference in molecular

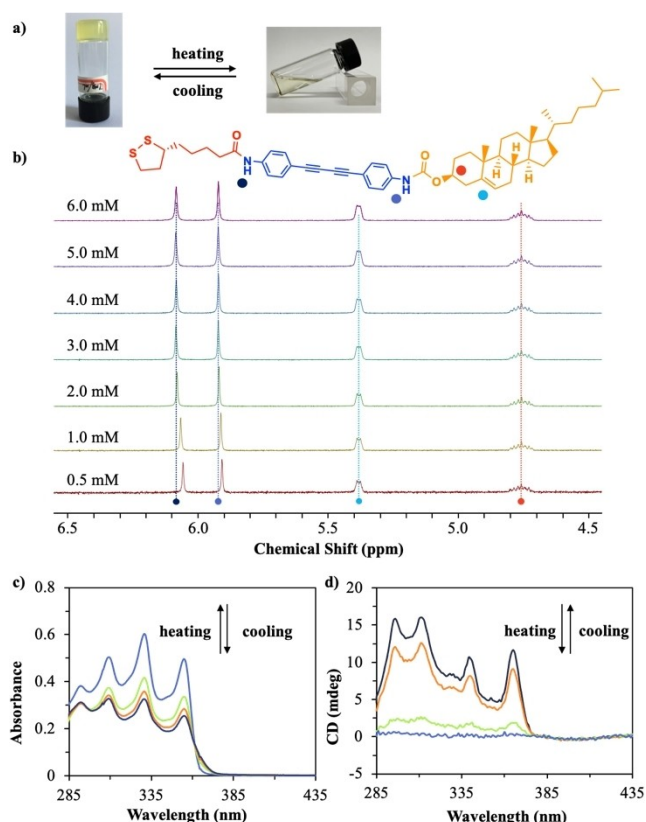


Figure 2. a) Photograph showing a reversible sol-gel transition of a LAC gel in *p*-xylene upon heating and cooling. b) Concentration-dependent ¹H NMR (400 MHz, toluene-*d*₆, 298 K) of LAC indicating the formation of intermolecular hydrogen bond. c) Temperature-dependent absorption spectra and d) CD spectra of LAC gel in *p*-xylene measured by using quartz cuvettes with a path length of 0.1 mm. The curves were recorded at 25, 45, 75 and 85 °C, respectively. The absorbance gradually decreased a little while positive CD signals gradually increased upon cooling.

alignment was supposed to cause the failure of **mLAC** to gel (Figure S13, SI). In generally, the driving force of gelation was mainly attributed to a synergetic effect of intermolecular hydrogen bond, strong Van der Waals force and π - π stacking. As hydrogen bond is sensitive to heat and can be rebuilt at low temperature, heating the gel will weaken the hydrogen bond and disintegrate the assemblies, whereas cooling brings out an opposite effect. This thermo reversible sol-gel transition always occurs in accompany with spectral changes. As shown in absorption spectra (Figure 2c), the decrease of absorbance as well as the bathochromic shift of absorption band edge were in accordance with gel formation when the temperature dropped.

Since both the lipoyl and cholesteryl substituents bear chiral centers, circular dichroism (CD) spectrum was used to study the optical activity of **LAC** gel formed in *p*-xylene. The molecular chirality of **LAC** is approximately absent in the region of 285–385 nm because the absorption of cholesterol falls in the range below 250 nm and the Cotton effect of lipoic acid is negligible due to its rather low extinction coefficient in the region tested (Figure S14, SI). However, strong supramolecular chirality was recorded after gelation of **LAC** (Figure 2d). It has been clarified in many reports^[32] that the self-assembly could cause the chirality transfer from the chiral groups to achiral moiety. In this case, Cotton effect with positive signals centered at 295 nm, 310 nm, 340 nm and 365 nm was exhibited due to the chirality transfer from chiral cholesterol and (*R*)- α -lipoic acid to DPDA moiety upon gelation. It should be pointed out that the CD signals originating from lipoic acid were considered to be negligible after comparing the CD signal intensities, and these four positive signals were in good agreement with the absorption peaks of DPDA moiety as shown in Figure 2c. Upon heating, the Cotton effect gradually decreased since the weakened hydrogen bond caused the disassembly of the gel and greatly hampered the chirality transfer, further proving the CD signals were induced by employment of hydrogen bond and molecular stacking. The Cotton effect of **LAC** gel in toluene and *o*-xylene was also observed (Figure S15a, SI). In addition, the CD spectra of **mLAC** and **LHC** in aromatic solvents were recorded and all the samples remained CD silent as expected, since no gelation was observed as mentioned above (Figure S15b and 15c, SI).

Molecular Alignment Study

Though lower than CGC, four CD signals appeared when the concentration increased from 0.75 mM to 1.0 mM, indicating that molecules have already started to assemble (Figure 3a). Meanwhile, one-dimensional nanofibrils of several micrometers in length and a few tens of nanometers in diameter were observed via field emission scanning electron microscope (FESEM, see Figure 3b). Upon further increasing the concentration to 3.0 mM, bathochromic shifts of 5 nm were clearly recorded in CD signals, suggesting a higher degree of π -conjugation and a better coplanarity. This spectral change reflected that the DPDA units aligned into a one-dimensional array of molecules for facilitating the topochemical progress

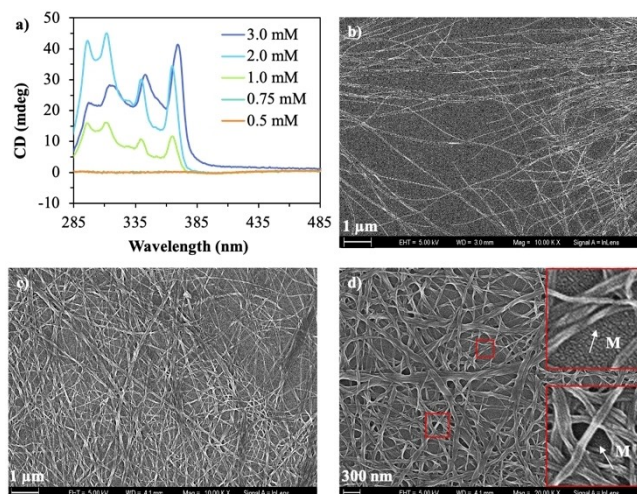


Figure 3. a) Concentration-dependent CD spectra of **LAC** gel in *p*-xylene measured in a quartz cuvette with a path length of 0.1 mm. FESEM images of nanofibrils prepared from samples at b) 1.0 mM, c) 2.0 mM and d) 3.0 mM by spin coating onto silicon wafers.

(Figure 3a). In this way, discrete helical nanofibrils intertwined with each other and assembled into a dense fibrous network as the concentration increased (Figure 3c and 3d), suggesting strong interfiber interactions. We believe that these findings may disclose a detailed assembly progression from the microscopic level to some extent.

Photopolymerization Initiated by 365-nm Irradiation

As discussed above, we've been successfully realized a great bathochromic shift of 20 nm in absorption bands compared with that of **LHC** and **mLAC**, along with the well-ordered pre-arrangement of monomers and through the gelation of **LAC**. A portable UV flashlight ($\lambda = 365$ nm, 5 W) was used then to initiate the topochemical reaction. Before irradiation, this white translucent gel only showed dim blue light under 365-nm illumination as indicated by the emission and excitation spectra (Figure 4a and S16, SI). Along with prolonging the irradiation time, a remarkable change in photoluminescence could be observed with the naked eye by giving out bright yellow light (Figure 4b, $\lambda_{\text{ex}} = 365$ nm).

During this process, a gradually increased emission intensity and a bathochromic shift can be clearly recorded (Figure 4c). The emission band centered at 475 nm shifted to 550 nm with the band edge extended to 725 nm or even longer. This dynamic progress reflected the progressive enlargement of π -conjugated skeleton upon photopolymerization. The reaction reached its equilibrium within 10 minutes while further prolonging the irradiation time to 30 minutes caused a slight hypsochromic shift again, probably due to the occurrence of photodegradation or photobleaching (Figure S17, SI). The efficiency can be further improved once an optimized light source could be applied. By altering the excitation wavelength, emission bands of various intensity or center wavelength were

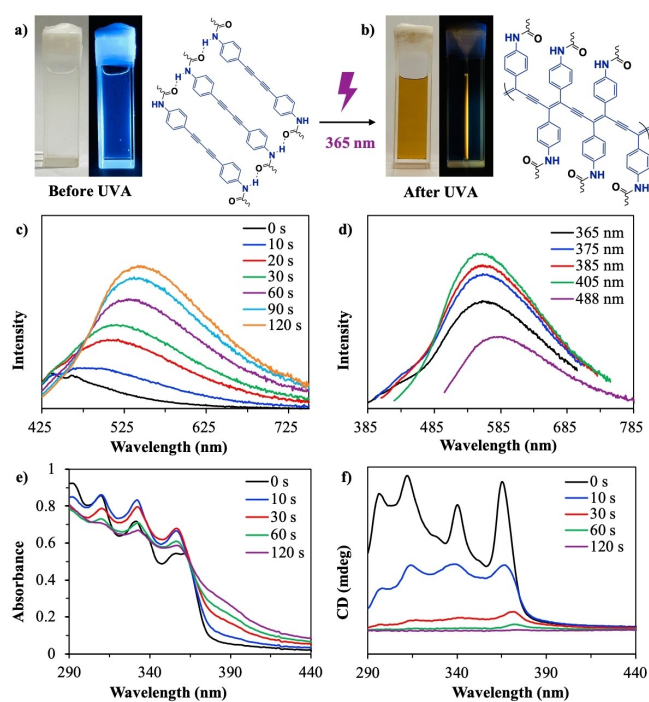


Figure 4. a–b) Photos of LAC gel (3.0 mM) in p-xylene with or without irradiation taken under day light or 365-nm light. Polymerization progress is monitored by c) emission spectra ($\lambda_{\text{ex}} = 405$ nm). d) The altering of excitation wavelength to 488 nm that to confirm the existence of high polymeric species after 10 min of irradiation. Polymerization progress monitored by e) absorption and f) CD spectra. Emission band centered at 550 nm and increase of absorption in the region of 370–440 nm both indicate a high degree of polymerization.

presented (Figure 4d and S18, SI). Since an enlarged π -conjugated structure, originating from a higher degree of polymerization, usually possesses a longer-wavelength excitation, a prominent emission band centered at 585 nm when excited by 488 nm clearly indicated the existence of high polymer species.

The reduced original absorption band of the monomer and the progressive increase of absorbance in the region of 370–440 nm (Figure 4e), resulting from the enlarged π -conjugated structure, also confirmed the photopolymerization process. Raman spectra showed that the peak at 2213 cm^{-1} attributed to the stretching of diacetylene was reduced after irradiation. Simultaneously, the formation of ene-yne unit associated with phenyl rings can be observed from the broad band centered at 1579 cm^{-1} (Figure S20, SI). In addition to the spectrometry methods, gel permeation chromatography results (Figure S19, SI) gave more solid evidence of the coexistence of polymer species with different degrees of polymerization from lower to higher. The number of repeating units was observed to exceed 10 in the highest molecular weight species. Thus, it can be concluded that this uniform gel network leads to a rather high degree of polymerization of diphenyldiacetylene-based fluorescent materials. As the polymerization proceeds, the originally stable gel began to disassemble. Therefore, CD signals gradually disappeared during the whole process, suggesting the polymerization occurred together with a loss of the gel network

(Figure 4f). Such disintegration process has been observed before, mainly attributed to a significant conformational change of bulky phenyl rings and the formation of π -conjugated skeleton disturbing the hydrogen bond network.^[18a,33] Similar to the cases reporting the enantioselective photopolymerization of aliphatic diacetylenes,^[34] the helical architecture in our case is definitely crucial to the bond-breaking and bond-making since the polymerization occurred along with a loss of chiral gel. As for the 2.0 mM and 1.0 mM samples, the rather loose stacking mode not only disturbed the chirality transfer, but hampered the polymerization also. Compared with 3.0 mM samples, after the same time of irradiation, emission bands at short wavelength when excited by 385 nm and below can be found. Due to a relatively weak π -electron delocalization, oligomers of DPDA derivatives usually possess emission bands at short wavelength, usually around 420 nm.^[19a,20a, 27b] The observed emission bands centered at 440 nm represented the formation of oligomeric species. Meanwhile, the relatively weak emission excited by 488 nm also indicated a lower content or absence of high polymers (Figure S21, SI). Of course, a THF solution of LAC resulted in an even less efficiency of the photopolymerization (only a little bit of oligomerization was indicated by a series of optical study, see Figure S22 and S23, SI).

Gel Transformation with Fluorescent Visualization

Thanks to such a longer-wavelength initiation, the topochemical reaction could be efficiently achieved in a glass vial. Figure 5a presents a series of photos captured from a time-lapse video (see Video, SI) recording the photopolymerization to visualize the transformation progress macroscopically. It should be noted that owing to the compact structure of gel, however, it was difficult for the light to penetrate a thick gel and the photopolymerization would be confined to the bottom (Figure S24, SI). Therefore, in order to reduce the effect of gel thickness, photopolymerization in an inverted quartz cuvette was carried out to picture the collapse of gel in motion. We can see that the yellow fluorescence extended from the edge to the center, which got brighter progressively upon irradiation. When the reaction went on to a certain extent, the hydrogen bond

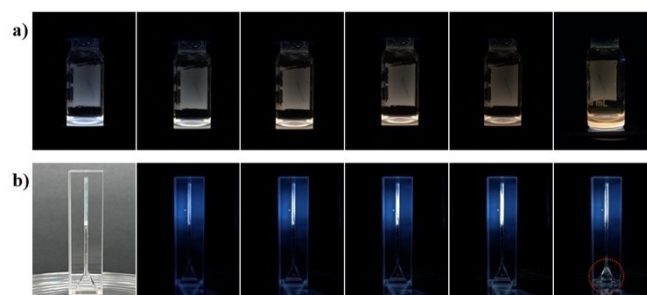


Figure 5. a) Images captured from a time-lapse video recording the photopolymerization process carried out in a glass vial irradiated by a 365 nm flashlight from the bottom. b) Images presenting the photopolymerization process of LAC gel in an inverted quartz cuvette with a path length of 1 mm irradiated by a 365-nm flashlight from the side.

network was disassembled and the gel collapsed to the ground as circled in Figure 5b. These results clearly visualized a gel transformation process along with the photopolymerization.

Conclusion

In summary, a universal strategy to rationally design fluorescent materials enabling a 365-nm light-initiated topochemical polymerization was demonstrated here. Through chemical modification of para-substituted amide groups on the phenyl rings, the absorption bands of DPDA moiety were rendered bathochromically shifted to longer wavelength. On this basis, in situ topochemical reaction initiated by 365 nm was successfully conducted upon the gelation of monomers. Intermolecular hydrogen bond plays a key role for pre-arrangement of the light-active reactants. The gel network composed of helical nanofibrils was believed to situate the reactive moiety in a serviceable position for facilitating the 1,4-addition polymerization, leading to a rather high degree of polymerization. This strategy, achieved under a rather mild conditions, could be monitored facilely by spectrometric methods as well as the naked eye, accompanied by a remarkable luminescence enhancement in response to the enlarged π -conjugated structure and the gel disassembly as the polymerization proceeds. We anticipate that the establishment of such a methodology could be valuable for further study on latent application of topochemical materials.

Experimental Section

General. Chemical reagents and solvents were all commercially available and used as received. ^1H NMR and ^{13}C NMR spectra were measured on a Bruker 400 MHz spectrometer. MS was measured by Matrix Assisted Laser Desorption Ionization-Time of Flight (MALDI-ToF) Mass Spectrometer (AB SCIEX 5800) using default Reflector Positive mode, with DCTB as the matrix. UV-vis absorption spectra were recorded in quartz cuvettes with a path length of 0.1 mm on a Shimadzu 1800 spectrophotometer. Emission spectra were taken in quartz cuvettes with a path length of 1 mm with an Edinburgh FLS1000 spectrofluorometer. Circular Dichroism (CD) spectra were recorded in quartz cuvettes with a path length of 0.1 mm on a Chirascan qCD. Raman spectra were recorded using XploRA Raman spectrometer. Field emission scanning electron microscope (FESEM) was performed on a Zeiss Gemini SEM500. Samples were prepared by spin coating onto silicon wafers and coated with a thin layer of Au to increase contrast. The polymeric species were analyzed with Agilent 1260 gel permeation chromatography (GPC) equipped with a UV detector and calibrated with polystyrene standard samples. THF was used as the eluent. See supporting information for the synthesis scheme pertaining to the compound labels.

Gelation in Organic Solvents. A typical procedure for gel formed in aromatic solvents including toluene, p-xylene and o-xylene is described as follows: LAC was suspended in the solvents in a sealed glass vial and gently heated at 80–90 °C until a transparent solution was obtained. After spontaneous cooling to room temperature, gel was formed with no gravitational flow upon inversion of the vial. To be specific, the concentration was 3 mM for p-xylene and 6 mM for toluene and o-xylene.

Photopolymerization. Photopolymerization was performed by irradiation with a UV flashlight ($\lambda = 365$ nm, 5 W) at a distance of 1 cm from the cell. The progress of the reaction was monitored by UV-vis spectra, emission spectra and CD spectra at different time intervals.

Synthesis of APDA ($\text{C}_{16}\text{H}_{12}\text{N}_2$). APDA was synthesized from 4-ethynylaniline according to a similar procedure described in the literature.^[35] ^1H NMR (400 MHz, DMSO- d_6 , 298 K): δ 7.23–7.18 (m, 4H), 6.55–6.51 (m, 4H), 5.73 (s, 4H). ^{13}C NMR (101 MHz, DMSO- d_6 , 298 K): δ 150.62, 133.99, 114.03, 106.86, 83.37, 72.48. MS (MALDI-ToF): calcd for $[\text{M}^+]$ $m/z = 232.10$, found m/z : 232.1772.

Synthesis of LA ($\text{C}_{24}\text{H}_{24}\text{N}_2\text{O}_5$). (*R*)- α -lipoic acid (0.2491 g, 1.2 mmol), HATU (0.4790 g, 1.3 mmol) and DIPEA (0.5 mL, 3 mmol) were dissolved in 20 mL DMF. After 30 min of pre-reaction at 0 °C, the mixed solution was added dropwise into APDA (0.2474 g, 1.1 mmol) solution in DMF (5 mL). The mixture was allowed to react at 45 °C for 4 h under N_2 . The solution was diluted with 100 mL chloroform and then washed by NaHCO_3 sat. solution, HCl and NaCl sat. solution in sequence. The organic layer was collected and dried by anhydrous Na_2SO_4 overnight. Compound LA was purified by silica gel chromatography (PE/EA = 4:1) to obtain yellow powder (0.2845 g, 61.5%). ^1H NMR (400 MHz, DMSO- d_6 , 298 K): δ 10.11 (s, 1H), 7.71–7.58 (m, 2H), 7.55–7.42 (m, 2H), 7.30–7.18 (m, 2H), 6.60–6.49 (m, 2H), 5.79 (s, 2H), 3.64 (dq, $J = 8.7, 6.2$ Hz, 1H), 3.24–3.08 (m, 2H), 2.42 (dt, $J = 18.5, 6.4$ Hz, 1H), 2.34 (t, $J = 7.3$ Hz, 2H), 1.94–1.82 (m, 1H), 1.76–1.52 (m, 4H), 1.41 (dt, $J = 14.1, 7.2$ Hz, 2H). ^{13}C NMR (101 MHz, DMSO- d_6 , 298 K): δ 171.90, 151.00, 140.71, 134.25, 133.34, 119.34, 115.52, 114.04, 106.14, 84.53, 81.48, 74.31, 71.89, 56.55, 40.39, 38.57, 36.77, 34.61, 28.78, 25.22. MS (MALDI-ToF): calcd for $[\text{M}^+]$ $m/z = 420.13$, found m/z : 420.2525.

Synthesis of LAC ($\text{C}_{52}\text{H}_{68}\text{N}_2\text{O}_5\text{S}_2$). The solution of LA (0.2104 g, 0.5 mmol), cholesteryl chloroformate (0.1690 g, 0.8 mmol) and Et_3N (0.5 mL, 3.6 mmol) in THF (10 mL) was refluxed overnight under N_2 . Solvent was removed by rotary evaporator, and pale-yellow powder was obtained (0.2196 g, 52.7%) through silica gel chromatography (PE/DCM = 1:1). ^1H NMR (400 MHz, DMSO- d_6 , 298 K): δ 10.12 (s, 1H), 9.93 (s, 1H), 7.65 (d, $J = 8.8$ Hz, 2H), 7.57–7.47 (m, 6H), 5.39 (s, 1H), 4.47 (dd, $J = 13.7, 9.1$ Hz, 1H), 3.68–3.58 (m, 1H), 3.15 (ddt, $J = 30.5, 11.0, 6.8$ Hz, 2H), 2.47–2.29 (m, 5H), 2.05–1.78 (m, 6H), 1.75–1.28 (m, 17H), 1.10 (dd, $J = 17.9, 9.6$ Hz, 6H), 0.97 (d, $J = 18.3$ Hz, 6H), 0.93–0.80 (m, 10H), 0.66 (s, 3H). ^{13}C NMR (101 MHz, CDCl_3 , 298 K): δ 170.98, 152.62, 139.42, 138.94, 138.59, 133.50, 133.39, 122.93, 119.33, 118.11, 117.29, 116.15, 81.51, 81.17, 75.33, 73.79, 73.42, 56.67, 56.37, 56.12, 49.98, 42.31, 40.28, 39.71, 39.52, 38.51, 38.40, 37.52, 36.93, 36.57, 36.18, 35.82, 34.64, 31.91, 31.86, 28.85, 28.25, 28.05, 28.03, 25.12, 24.30, 23.85, 22.85, 22.59, 21.05, 19.35, 18.73, 11.88. MS (MALDI-ToF): calcd for $[\text{M} + \text{K}]^+$ $m/z = 871.43$, found m/z : 871.2699.

Synthesis of mAPDA ($\text{C}_{16}\text{H}_{12}\text{N}_2$). mAPDA was synthesized from 3-ethynylaniline in the same way as APDA. ^1H NMR (400 MHz, DMSO- d_6 , 298 K): δ 7.06 (t, $J = 7.8$ Hz, 2H), 6.71 (dt, $J = 2.3, 1.5$ Hz, 4H), 6.66 (ddd, $J = 8.1, 2.2, 1.0$ Hz, 2H), 5.32 (s, 4H). ^{13}C NMR (101 MHz, DMSO- d_6 , 298 K): δ 149.37, 129.85, 121.14, 120.21, 117.09, 116.16, 82.77, 72.83. MS (MALDI-ToF): calcd for $[\text{M}^+]$ $m/z = 232.10$, found m/z : 232.0432.

Synthesis of mLAC ($\text{C}_{52}\text{H}_{68}\text{N}_2\text{O}_5\text{S}_2$). Synthetic route of mLAC was similar to that of LAC except for the starting compound mAPDA. After reaction of mAPDA with (*R*)- α -lipoic acid and cholesteryl chloroformate successively, white powder mLAC was obtained through silica gel chromatography (PE/EA = 4:1). ^1H NMR (400 MHz, DMSO- d_6 , 298 K): δ 10.07 (s, 1H), 9.85 (s, 1H), 7.90 (s, 1H), 7.72–7.54 (m, 3H), 7.31 (ddd, $J = 26.1, 17.3, 7.9$ Hz, 4H), 5.40 (s, 1H), 4.48 (s, 1H), 3.64 (td, $J = 12.1, 6.1$ Hz, 1H), 3.25–3.08 (m, 2H), 2.45–2.30 (m,

5H), 2.01–1.77 (m, 6H), 1.71–1.29 (m, 17H), 1.10 (d, $J=18.7$ Hz, 6H), 0.98 (d, $J=17.1$ Hz, 6H), 0.94–0.82 (m, 10H), 0.67 (s, 3H). ^{13}C NMR (101 MHz, CDCl_3 , 298 K): δ 171.00, 152.85, 139.49, 138.22, 137.95, 129.22, 128.38, 127.44, 123.30, 122.88, 122.40, 122.09, 120.79, 119.53, 81.34, 81.09, 75.26, 74.14, 73.95, 56.68, 56.37, 56.12, 49.99, 42.32, 40.27, 39.73, 39.52, 38.51, 38.41, 37.45, 36.95, 36.58, 36.19, 35.81, 34.66, 31.92, 31.87, 28.85, 28.25, 28.06, 28.03, 25.16, 24.30, 23.84, 22.85, 22.58, 21.07, 19.35, 18.73, 11.88. MS (Maldi-ToF): calcd for $[\text{M}+\text{K}]^+$ $m/z=871.43$, found m/z : 871.3015; $[\text{M}+\text{Na}]^+=855.46$, found $m/z=855.3115$.

Synthesis of HPDA ($\text{C}_{16}\text{H}_{10}\text{O}_2$). HPDA was synthesized according to the procedure described in the literature.^[36] ^1H NMR (400 MHz, $\text{DMSO}-d_6$, 298 K): δ 10.13 (s, 2H), 7.41 (d, $J=8.8$ Hz, 4H), 6.79 (d, $J=8.8$ Hz, 4H). ^{13}C NMR (101 MHz, $\text{DMSO}-d_6$, 298 K): δ 159.36, 134.57, 116.38, 111.18, 82.29, 72.76. MS (Maldi-ToF): calcd for $[\text{M}]^+$ $m/z=234.07$, found m/z : 234.2119.

Synthesis of LHC ($\text{C}_{52}\text{H}_{66}\text{O}_5\text{S}_2$). Synthetic route of LHC was similar to that of LAC except for the starting compound HPDA. After reaction of HPDA with (*R*)- α -lipoic acid and cholesteryl chloroformate successively, white powder LHC was obtained through silica gel chromatography (PE/DCM=2:1). ^1H NMR (400 MHz, CDCl_3 , 298 K): δ 7.53 (dd, $J=6.6, 4.7$ Hz, 4H), 7.18 (d, $J=8.7$ Hz, 2H), 7.07 (d, $J=8.6$ Hz, 2H), 5.43 (s, 1H), 4.58 (dt, $J=10.5, 5.1$ Hz, 1H), 3.60 (dt, $J=13.0, 6.5$ Hz, 1H), 3.25–3.08 (m, 2H), 2.59 (t, $J=7.3$ Hz, 2H), 2.54–2.41 (m, 3H), 2.07–1.83 (m, 6H), 1.81–1.59 (m, 7H), 1.52–1.40 (m, 5H), 1.33 (dd, $J=22.6, 15.4$ Hz, 5H), 1.18–1.09 (m, 6H), 1.05–0.97 (m, 6H), 0.92 (d, $J=6.5$ Hz, 3H), 0.86 (dd, $J=6.6, 1.7$ Hz, 7H), 0.68 (s, 3H). ^{13}C NMR (101 MHz, CDCl_3 , 298 K): δ 171.52, 152.42, 151.58, 151.23, 139.02, 133.78, 133.76, 123.32, 121.90, 121.37, 119.38, 119.27, 80.86, 80.71, 79.22, 74.01, 73.91, 56.67, 56.29, 56.11, 49.96, 42.32, 40.26, 39.70, 39.52, 38.54, 37.90, 36.81, 36.55, 36.18, 35.80, 34.61, 34.13, 31.92, 31.83, 28.71, 28.24, 28.03, 27.62, 24.57, 24.29, 23.83, 22.85, 22.58, 21.06, 19.30, 18.73, 11.88. MS (Maldi-ToF): calcd for $[\text{M}+\text{K}]^+$ $m/z=874.18$, found m/z : 874.4517.

Acknowledgements

This work was financially supported by 2019 NSFC (21975046) and partially from the National Key Research and Development Program of China (2017YFA0207700).

Conflict of Interest

The authors declare no conflict of interest.

Keywords: diphenyldiacetylene · topochemical polymerization · organogel · hydrogen bond · fluorescent materials

- [1] a) X. Sun, T. Chen, S. Huang, L. Li, H. Peng, *Chem. Soc. Rev.* **2010**, *39*, 4244–4257; b) A. Sarkar, S. Okada, H. Matsuzawa, H. Matsuda, H. Nakanishi, *J. Mater. Chem.* **2000**, *10*, 819–828.
[2] a) B. P. Krishnan, S. Mukherjee, P. M. Aneesh, M. A. Namboothiry, K. M. Sureshan, *Angew. Chem. Int. Ed. Engl.* **2016**, *55*, 2345–2349; b) M. Ulaganathan, R. V. Hansen, N. Drayton, H. Hingorani, R. G. Kutty, H. Joshi, S. Sreejith, Z. Liu, J. Yang, Y. Zhao, *ACS Appl. Mater. Interfaces* **2016**, *8*, 32643–32648; c) S. Cho, G. Han, K. Kim, M. M. Sung, *Angew. Chem. Int. Ed.* **2011**, *50*, 2742–2746; *Angew. Chem.* **2011**, *123*, 2794–2798.

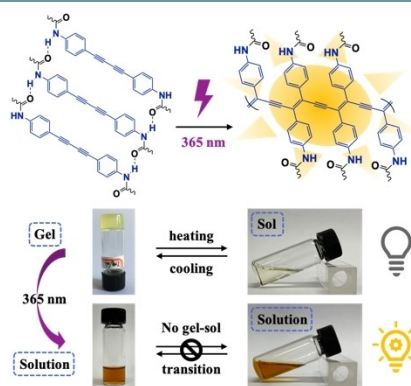
- [3] a) H. Jiang, X. Y. Hu, S. Schlesiger, M. Li, E. Zellermann, S. K. Knauer, C. Schmuck, *Angew. Chem. Int. Ed. Engl.* **2017**, *56*, 14526–14530; b) Y. K. Jung, M. A. Woo, H. T. Soh, H. G. Park, *Chem. Commun.* **2014**, *50*, 12329–12332.
[4] a) Y. K. Jung, C. Jung, H. G. Park, *ACS Appl. Mater. Interfaces* **2016**, *8*, 15684–15690; b) D. J. Ahn, J. M. Kim, *Acc. Chem. Res.* **2008**, *41*, 805–816.
[5] Y. J. Choi, S. Park, W. J. Yoon, S. I. Lim, J. Koo, D. G. Kang, S. Park, N. Kim, K. U. Jeong, *Adv. Mater.* **2020**, *32*, 2003980.
[6] J. Lee, S. Seo, J. Kim, *ACS Appl. Mater. Interfaces* **2018**, *10*, 3164–3169.
[7] a) S. Kim, S. Lee, T. F. Anjong, H. Y. Jang, J. Y. Kim, C. Lee, S. Park, H. J. Lee, J. Yoon, J. Kim, *J. Phys. Chem. C* **2016**, *120*, 28407–28414; b) L. Xia, B. F. Cheng, T. Y. Zeng, X. Nie, G. Chen, Z. Zhang, W. J. Zhang, C. Y. Hong, Y. Z. You, *Adv. Sci.* **2020**, *7*, 1902451.
[8] a) N. Pootrakulchote, C. Reanprayoon, J. Gasiorowski, N. S. Sariciftci, P. Thamyongkit, *New J. Chem.* **2015**, *39*, 9228–9233; b) M. A. Desta, C.-W. Liao, S.-S. Sun, *Chem. Asian J.* **2017**, *12*, 690–697; c) J. Nishide, T. Oyamada, S. Akiyama, H. Sasabe, C. Adachi, *Adv. Mater.* **2006**, *18*, 3120–3124.
[9] a) X. Chen, G. Zhou, X. Peng, J. Yoon, *Chem. Soc. Rev.* **2012**, *41*, 4610–4630; b) S. Lee, J. Y. Kim, X. Chen, J. Yoon, *Chem. Commun.* **2016**, *52*, 9178–9196; c) H. N. Kim, Z. Guo, W. Zhu, J. Yoon, H. Tian, *Chem. Soc. Rev.* **2011**, *40*, 79–93.
[10] a) O. Yarimaga, J. Jaworski, B. Yoon, J. M. Kim, *Chem. Commun.* **2012**, *48*, 2469–2485; b) D. H. Park, J. Hong, I. S. Park, C. W. Lee, J. M. Kim, *Adv. Funct. Mater.* **2014**, *24*, 5186–5193; c) S. Chae, J. P. Lee, J. M. Kim, *Adv. Funct. Mater.* **2016**, *26*, 1769–1776.
[11] a) X. Qian, B. Städler, *Adv. Funct. Mater.* **2020**, *30*, 2004605; b) X. M. Qian, C. Gargalo, K. V. Gernaey, B. Stadler, *ACS Appl. Nano Mater.* **2020**, *3*, 3439–3448; c) X. M. Qian, B. Stadler, *Chem. Mater.* **2019**, *31*, 1196–1222.
[12] G. Wegner, *J. Polym. Sci., Part B: Polym. Lett.* **1971**, *9*, 133–144.
[13] Z. Li, F. W. Fowler, J. W. Lauher, *J. Am. Chem. Soc.* **2008**, *131*, 634–643.
[14] a) L. Zhong, X. Zhu, P. Duan, M. Liu, *J. Phys. Chem. B* **2010**, *114*, 8871–8878; b) X. Huang, M. Liu, *Chem. Commun.* **2003**, 66–67; c) Y. Xu, J. Li, W. Hu, G. Zou, Q. Zhang, *J. Colloid Interface Sci.* **2013**, *400*, 116–122.
[15] a) Y. Xu, M. D. Smith, M. F. Geer, P. J. Pellechia, J. C. Brown, A. C. Wibowo, L. S. Shimizu, *J. Am. Chem. Soc.* **2010**, *132*, 5334–5335; b) W. W. L. Xu, M. D. Smith, J. A. Krause, A. B. Greytak, S. G. Ma, C. M. Read, L. S. Shimizu, *Cryst. Growth Des.* **2014**, *14*, 993–1002; c) J. W. Lauher, F. W. Fowler, N. S. Goroff, *Acc. Chem. Res.* **2008**, *41*, 1215–1229.
[16] a) J. Y. Chang, J. R. Yeon, Y. S. Shin, M. J. Han, S. K. Hong, *Chem. Mater.* **2000**, *12*, 1076–1082; b) Y. Xu, H. Jiang, Q. Zhang, F. Wang, G. Zou, *Chem. Commun.* **2014**, *50*, 365–367.
[17] a) F. L. Wu, N. V. S. D. K. Bhupathiraju, A. Brown, Z. T. Liu, C. M. Drain, J. D. Batteas, *J. Phys. Chem. C* **2020**, *124*, 4081–4089; b) F. Xie, C. F. Chen, J. Chen, M. H. Liu, *J. Photochem. Photobiol. A* **2018**, *355*, 283–289; c) Y. H. Chan, J. T. Lin, I. W. Chen, C. H. Chen, *J. Phys. Chem. B* **2005**, *109*, 19161–19168.
[18] a) J. R. Neabo, K. I. Tohondjona, J. F. Morin, *Org. Lett.* **2011**, *13*, 1358–1361; b) G. Wang, N. Goyal, H. P. Mangunuru, H. Yang, S. Cheuk, P. V. Reddy, *J. Org. Chem.* **2015**, *80*, 733–743; c) Y. J. Choi, D. Jung, S. I. Lim, W. J. Yoon, D. Y. Kim, K. U. Jeong, *ACS Appl. Mater. Interfaces* **2020**, *12*, 33239–33245; d) Y. Xu, S. Fu, F. Liu, H. Yu, J. Gao, *Soft Matter* **2018**, *14*, 8044–8050; e) S. R. Diegelmann, N. Hartman, N. Markovic, J. D. Tovar, *J. Am. Chem. Soc.* **2012**, *134*, 2028–2031; f) S. Li, L. Zhang, J. Jiang, Y. Meng, M. Liu, *ACS Appl. Mater. Interfaces* **2017**, *9*, 37386–37394.
[19] a) L. Zhu, M. T. Trinh, L. Yin, Z. Zhang, *Chem. Sci.* **2016**, *7*, 2058–2065; b) L. L. Zhu, X. Li, S. N. Sanders, H. Agren, *Macromolecules* **2015**, *48*, 5099–5105; c) M. J. Zhu, L. Y. Yin, Y. Y. Zhou, H. W. Wu, L. L. Zhu, *Macromolecules* **2018**, *51*, 746–754; d) S. Rondeau-Gagne, J. R. Neabo, M. Desroches, J. Larouche, J. Brisson, J. F. Morin, *J. Am. Chem. Soc.* **2013**, *135*, 110–113; e) J. Q. Fan, X. Xu, W. Yu, Z. H. Wei, D. Q. Zhang, *Polym. Chem.* **2020**, *11*, 1947–1953; f) M. N. Tahir, A. Nyayachavadi, J. F. Morin, S. Rondeau-Gagne, *Polym. Chem.* **2018**, *9*, 3019–3028.
[20] a) Y. I. Fujiwara, K. Kadota, S. S. Nagarkar, N. Tabori, S. Kitagawa, S. Horike, *J. Am. Chem. Soc.* **2017**, *139*, 13876–13881; b) N. Kameta, W. Ding, M. Masuda, *Chem. Commun.* **2021**, 57, 464–467.
[21] a) L. Zhu, H. Tran, F. L. Beyer, S. D. Walck, X. Li, H. Agren, K. L. Killops, L. M. Campos, *J. Am. Chem. Soc.* **2014**, *136*, 13381–13387; b) D. Krishnan, R. B. A. Raj, E. B. Gowd, *Polym. Chem.* **2019**, *10*, 3154–3162.
[22] J. P. Huo, Q. J. Deng, T. Fan, G. Z. He, X. H. Hu, X. X. Hong, H. Chen, S. H. Luo, Z. Y. Wang, D. C. Chen, *Polym. Chem.* **2017**, *8*, 7438–7445.
[23] G. Shin, M. I. Khazi, J.-M. Kim, *Macromolecules* **2019**, *53*, 149–157.
[24] M. N. Tahir, E. Abdulhamied, A. Nyayachavadi, M. Selivanova, S. H. Eichhorn, S. Rondeau-Gagne, *Langmuir* **2019**, *35*, 15158–15167.

- [25] a) E. Jahnke, I. Lieberwirth, N. Severin, J. P. Rabe, H. Frauenrath, *Angew. Chem. Int. Ed. Engl.* **2006**, *45*, 5383–5386; b) P. Tanphibal, K. Tashiro, S. Chirachanchai, *Macromol. Rapid Commun.* **2016**, *37*, 685–690; c) Y. Meng, J. Jiang, M. Liu, *Nanoscale* **2017**, *9*, 7199–7206; d) S. M. Curtis, N. Le, F. W. Fowler, J. W. Lauher, *Cryst. Growth Des.* **2005**, *5*, 2313–2321.
- [26] Y. Lu, Y. Yang, A. Sellinger, M. Lu, J. Huang, H. Fan, R. Haddad, G. Lopez, A. R. Burns, D. Y. Sasaki, J. Shelnutt, C. J. Brinker, *Nature* **2001**, *410*, 913–917.
- [27] a) S. Wu, L. Pan, Y. Huang, N. Yang, Q. Zhang, *Soft Matter* **2018**, *14*, 6929–6937; b) X. Y. Jia, M. J. Zhu, Q. Bian, B. B. Yue, Y. P. Zhuang, B. Wu, L. Yu, J. D. Ding, J. J. Zhang, L. L. Zhu, *Macromolecules* **2018**, *51*, 8038–8045.
- [28] a) Y. Wang, L. Li, K. Yang, L. A. Samuelson, J. Kumar, *J. Am. Chem. Soc.* **2007**, *129*, 7238–7239; b) S. Wang, Y. Li, H. Liu, J. Li, T. Li, Y. Wu, S. Okada, H. Nakanishi, *Org. Biomol. Chem.* **2015**, *13*, 5467–5474.
- [29] a) D. A. Stone, L. Hsu, N. R. Wheeler, E. Wilusz, W. Zukas, G. E. Wnek, L. T. J. Korley, *Soft Matter* **2011**, *7*, 2449–2455; b) M. H. Liu, G. H. Ouyang, D. Niu, Y. T. Sang, *Org. Chem. Front.* **2018**, *5*, 2885–2900; c) P. Xing, H. Chen, L. Bai, A. Hao, Y. Zhao, *ACS Nano* **2016**, *10*, 2716–2727; d) S. Shinkai, K. Murata, *J. Mater. Chem.* **1998**, *8*, 485–495.
- [30] a) R. Mohanrao, K. Hema, K. M. Sureshan, *ACS Appl. Polym. Mater.* **2020**, *2*, 4985–4992; b) B. P. Krishnan, S. Raghu, S. Mukherjee, K. M. Sureshan, *Chem. Commun.* **2016**, *52*, 14089–14092.
- [31] a) B. P. Krishnan, K. M. Sureshan, *J. Am. Chem. Soc.* **2017**, *139*, 1584–1589; b) B. P. Krishnan, S. Ramakrishnan, K. M. Sureshan, *Chem. Commun.* **2013**, *49*, 1494–1496.
- [32] a) L. Zhang, T. Wang, Z. Shen, M. Liu, *Adv. Mater.* **2016**, *28*, 1044–1059; b) M. Liu, L. Zhang, T. Wang, *Chem. Rev.* **2015**, *115*, 7304–7397; c) P. Duan, H. Cao, L. Zhang, M. Liu, *Soft Matter* **2014**, *10*, 5428–5448.
- [33] O. J. Dautel, M. Robitzer, J. P. Lere-Porte, F. Serein-Spirau, J. J. Moreau, *J. Am. Chem. Soc.* **2006**, *128*, 16213–16223.
- [34] a) J. Kim, J. Lee, W. Y. Kim, H. Kim, S. Lee, H. C. Lee, Y. S. Lee, M. Seo, S. Y. Kim, *Nat. Commun.* **2015**, *6*, 6959; b) Y. Xu, G. Yang, H. Xia, G. Zou, Q. Zhang, J. Gao, *Nat. Commun.* **2014**, *5*, 5050; c) C. He, Z. Feng, S. Shan, M. Wang, X. Chen, G. Zou, *Nat. Commun.* **2020**, *11*, 1188; d) C. Chen, J. Chen, T. Wang, M. Liu, *ACS Appl. Mater. Interfaces* **2016**, *8*, 30608–30615.
- [35] I. Yamaguchi, H. Higashi, S. Kimura, M. Sato, *Helv. Chim. Acta* **2010**, *93*, 819–828.
- [36] J. Park, E. Park, A. Kim, S. A. Park, Y. Lee, K. W. Chi, Y. H. Jung, I. S. Kim, *J. Org. Chem.* **2011**, *76*, 2214–2219.

Manuscript received: April 30, 2021
 Revised manuscript received: May 29, 2021
 Accepted manuscript online: June 1, 2021
 Version of record online: ■■■, ■■■■

FULL PAPER

A universal strategy to rationally design diphenyldiacetylene-based fluorescent materials enabling a 365-nm light-initiated topochemical polymerization is demonstrated here. Through chemical modification of para-substituted amide groups and construction of gel networks, the reaction featured a remarkably progressive luminescence enhancement and gel disassembly upon irradiation, leading to a rather high degree of polymerization.



*M. Zhu, Prof. L. Zhu**

1 – 8

Rational Design of Diphenyldiacetylene-Based Fluorescent Materials Enabling a 365-nm Light-Initiated Topochemical Polymerization

